2 Neutrinoless double beta decay and lepton flavor violation in left-right symmetric model

In this chapter, we have studied neutrinoless double beta decay and charged lepton flavor violation in broken $\mu-\tau$ symmetric neutrino masses in a generic left-right symmetric model (LRSM). We considered the leading order $\mu-\tau$ symmetric neutrino mass matrix to be originating from the type I (II) seesaw mechanism, while on the contrary, the perturbations to $\mu-\tau$ symmetry in order for generation of non-zero reactor mixing angle, θ_{13} as required by latest neutrino oscillation data, originates from the type II (I) seesaw mechanism. We considered the widely studied four different realizations of $\mu-\tau$ symmetry, viz. Tri-bimaximal mixing (TBM), bi-maximal mixing (BM), hexagonal mixing (HM) and golden ratio mixing (GRM). We then studied the new physics contributions to neutrinoless double beta decay (NDBD) ignoring the left-right gauge boson mixing and the heavy-light neutrino mixing within the framework of LRSM. We have considered the mass of the gauge bosons and scalars to be around TeV and studied the effects of the new physics contributions on the effective mass and the NDBD half-life and compared with the current experimental limit imposed by the KamLAND-Zen experiment. We further extended our analysis by correlating the lepton flavor violation of the decay processes, $\mu \to 3e$ and $\mu \to e\gamma$ with the lightest neutrino mass and atmospheric mixing angle θ_{23} respectively.

2.1 Introduction

The milestone discovery of neutrino oscillation and the corresponding realization that neutrinos are massive particles and they mix during propagation has been one of the compelling revelation which suggests physics beyond the most successful Standard Model (SM) of particle physics. That neutrinos have non-zero but tiny masses and large mixing has been well established by several neutrino experiments [1, 2, 3, 4, 5, 6, 7, 8, 9] during the last two decades. Among the above-mentioned experiments, the relatively recent ones like T2K [5], Double Chooz [6], Daya Bay [7], RENO [8] and MINOS [9] experiments have not only confirmed the results from earlier observations but also discovered the non-zero reactor mixing angle θ_{13} and the other neutrino parameters more accurately. We refer to the following 3σ global fit values of the neutrino oscillation parameters as shown in the table 2.1 for this work.

PARAMETERS	3σ RANGES	BEST FIT$\pm1\sigma$
$\Delta m^2_{21}[10^-5\text{eV}^2]$	7.11-8.18	$7.60^{+0.19}_{-0.18}$
$\Delta m^2_{31}[10^-3\text{eV}^2]$(NH)	2.30-2.65	$2.48^{+0.05}_{-0.07}$
$\Delta m^2_{23}[10^-3\text{eV}^2]$(IH)	2.26-2.48	$2.38^{+0.05}_{-0.06}$
$\sin^2\theta_{12}$	0.278-0.375	0.323±0.016
$\sin^2\theta_{23}$(NH)	0.392-0.643	$0.567^{+0.032}_{-0.128}$
(IH)	$0.403-0.640$	$0.573^{+0.025}_{-0.043}$
$\sin^2\theta_{13}$(NH)	0.177-0.294	0.234 ± 0.020
(IH)	$0.183-0.297$	0.240± 0.019
δ	0-2π(NH)	254^0
	0-2π(IH)	266^0

Table 2.1: Global fit 3σ values of ν oscillation parameters [10]

Notwithstanding, the absolute neutrino mass scale is still unperceived. However, the Planck experiment has given an upper bound on the sum of the light neutrino mass to be $\sum_\text{i}|\text{m}_\text{i}|$ <0.23 eV [11] in 2012 and recently the bound has been constrained to $\sum_\text{i}|\text{m}_\text{i}|$ <0.17 eV [12]. The simplest hypothesis (way) to account for a neutrino mass is to introduce atleast two right-handed (RH) neutrino in the SM. This will allow a Dirac coupling with the Higgs, like other fermions in the SM. However, corresponding Yukawa coupling has to be fine tuned around 10^{-12} which is quite unnatural. This kind of fine tuning can be avoided to explain the neutrino masses in the seesaw mechanism, a mechanism beyond SM (BSM) physics which is categorized into type I [13, 14, 15], type II [16, 17, 18], type III [19, 20], inverse [21, 22] seesaw mechanism. The BSM physics also unveils various phenomenon like baryon asymmetry of the universe (BAU), lepton number violation (LNV), lepton flavor violation (LFV), existence of dark matter etc. One of the theoretical framework to make the first three processes observable is the left-right symmetric model (LRSM) [23, 24, 25, 26, 27, 28] which is considered to be an appealing candidate for physics BSM. Here, the gauge group is very simple extension of the SM gauge group. It provides a natural framework to understand the spontaneous breaking of parity and origin of small neutrino mass via seesaw mechanism.

Furthermore, the physics community worldwide is embarking on the next challenging problem in finding out the nature of the neutrinos, whether they are four component Dirac particles possessing a conserved lepton number or two component Majorana particles, along with the absolute scale of neutrino mass. This problem is directly related to the issue of LN conservation, which is one of the most obscure sides of the SM not supported by an underlying principle. One of such process of fundamental importance in particle physics which pops up almost in any extension of the SM is neutrinoless double beta decay (NDBD) [29, 30] in which there is a violation of total lepton number conservation by two units. Its existence is directly linked to that of the Majorana neutrinos [31] (i.e., identical to its own anti particle). The general expression for the total decay width of $0\nu\beta\beta$ by considering the interaction of the electrons and the final nucleus is given by,

$$\Gamma^{0\nu} = \frac{1}{\mathrm{T}_{\frac{1}{2}}{}^{0\nu}} = \mathrm{G}^{0\nu}(\mathrm{Q},\mathrm{Z})\left|\mathrm{M}^{0\nu}\right|^2 \frac{|\mathrm{m}_{\beta\beta}|^2}{\mathrm{m_e}^2}. \tag{2.1}$$

The numerical values of $\mathrm{G}^{0\nu}(\mathrm{Q},\mathrm{Z})$, Q and the natural abundance of several nuclei of experimental interest are given in the table 2.2 which are adopted from reference [32].

The main aim of the experiment on the search for $0\nu\beta\beta$ decay is the measurement of the effective Majorana neutrino mass, which is a combination of the neutrino mass eigenstates and neutrino mixing matrix terms, given by,

$\beta\beta - decay$	$G^{0\nu}[10^{-14}y^{-1}$	Q$[KeV]$	Experiments
$48_{Ca} \to 48_{Ti}$	6.3	4273.7	CANDLES
$76_{Ge} \to 76_{Se}$	0.63	2039.1	GERDA, Majorana
$82_{Se} \to 82_{Kr}$	2.7	2995.5	SuperNEMO, Lucifer
$100_{Mo} \to 100_{Ru}$	4.4	3035.0	MOON, AMoRe
$116_{Cd} \to 116_{Sn}$	4.6	2809	Cobra
$130_{Te} \to 130_{Xe}$	4.1	2530.3	CUORE
$136_{Xe} \to 136_{Ba}$	4.3	2461.9	EXO, KamLAND-Zen, NEXT, XMASS
$150_{Nd} \to 150_{Sm}$	19.2	3367.3	SNO+, DCBA/MTD

Table 2.2: The values of $\mathrm{G}^{0\nu}(\mathrm{Q},\mathrm{Z})$, Q of the initial isotope for several NDBD processes of experimental interest.

$$\mathrm{m}_{\beta\beta} = \sum_{\mathrm{j}} \mathrm{U_{ej}}^2 \mathrm{m_j}, \mathrm{j} = 1, 2, 3, \tag{2.2}$$

where, $\mathrm{U_{ej}}$ are the elements of the first row of the neutrino mixing matrix, $\mathrm{U_{PMNS}}$ (dependent on the known parameters θ_{13}, θ_{12} and the unknown Majorana phases α and β [33]) as defined in equation 1.28. In the standard parameterization of the mixing matrix, $\mathrm{m}_{\beta\beta}$ is given by,

$$\mathrm{m}_{\beta\beta} = \mathrm{m_1 c_{12}^2 c_{13}^2 + m_2 s_{12}^2 c_{13}^2 e^{2i\alpha} + m_3 s_{13}^2 e^{2i\beta}}. \tag{2.3}$$

A huge amount of experimental and theoretical activity is pursued in order to detect and predict the decay process. Although no convincing experimental evidence of the decay exists till date, but new generation of experiments that are already running or about to run assures to expedite the current limits exploring the degenerate-hierarchy region of neutrino masses. In addition, from the life time of this decay combined with sufficient knowledge of the nuclear matrix elements (NME), one can set a constraint involving the neutrino masses. Moreover, if one incorporates the recent results of neutrino oscillation experiments, one can set a stringent limit on the neutrino mass scale. The latest experiments [35, 36] that have improved the lower bound of the half-life of the decay process include KamLAND-Zen [37] and GERDA [38] which uses Xenon-136 and Germanium-76 nuclei respectively. Incorporating the results from first and second phase of the experiment, KamLAND-Zen imposes the best lower limit on the decay half-life using Xe-136 as $\mathrm{T}^{0\nu}_{1/2} > 1.07 \times 10^{26}$ yr at 90% CL and the corresponding upper limit of effective Majorana mass in the range (0.061-0.165)eV.

Again it is utmost important to identify the possible underlying symmetries in order to understand the origin of the tiny neutrino mass and the large leptonic mixing. Symmetries provides relations among two or more free parameters of the model or can even make them vanish thereby making the model more predictive. The $\mu - \tau$ symmetric [67, 68, 69, 70, 72, 73, 75, 76, 77, 78] neutrino mass matrix giving zero θ_{13} which are widely studied is one such framework where discrete flavor symmetries relates two or more terms in the neutrino mass matrix. The neutrino oscillation data before the discovery of non-zero reactor mixing angle, θ_{13} perfectly agrees with $\mu - \tau$ symmetric neutrino mass matrix. The four different realizations of neutrino mixing pattern generally found in literature which can generate from μ-τ symmetric mass matrices are namely, tri-bimaximal mixing (TBM), bimaximal mixing (BM), hexagonal mixing (HM) and golden ratio mixing (GRM) matrices. But, after discovery of non-zero θ_{13}, one needs to go beyond these μ-τ symmetric framework. Since the experimental value of θ_{13} is much smaller in comparison to the other two mixing angles, μ-τ symmetry can still be a reasonable approximation and the non-zero θ_{13} [49] can be obtained by including the presence of small perturbation to μ-τ symmetry.

The discovery of neutrino oscillation has provided clear evidence of the fact that neutrinos are massive as well as the violation of the lepton flavor [50, 51] during the propagation of the neutrinos. Lepton flavor is consequently a broken symmetry and the SM has to be adapted to incorporate massive neutrinos and thus we can also hope that lepton flavor violation (LFV) will be visible in the charged lepton sector [157]. The exact mechanism of LFV being unknown, its study is of large interest as it is linked to neutrino mass generation, CP violation and new physics BSM. The LFV effects from new particles at TeV scale are naturally generated in many models and therefore considered to be a prominent signature for new physics. In LRSM, where electroweak symmetry is broken dynamically, an experimentally accessible amount of LFV is predicted in a large region of parameter space. In a wide range of models for physics BSM, highest sensitivity in terms of BR is expected for $\mu \to 3e$ and $\mu \to e\gamma$ decay processes.

To study these phenomenon theoretically or phenomenologically, many works have been performed in LRSM based framework [53, 54, 55, 56, 57, 58, 59, 60, 61]. In most of these works, authors mostly considered the TBM like neutrino mass as leading order contribution and arising from type I seesaw and using the type II seesaw as a perturbation to generate non-zero θ_{13} [62, 63]. More recently, the authors of [64] [65] studied the new physics contribution to NDBD with prominent type I and type II as well as equally dominating type I and type II seesaw. Again, many works have been done in charged lepton flavor violation sector in literature considering type I and type II dominant cases as well as equally dominant type I and type II in the TeV scale LRSM framework which is within the presently accessible reach of the colliders and implements the two seesaw mechanisms naturally [52].

In this context, we present a phenomenological study of different $\mu-\tau$ symmetric [67, 68, 69, 70, 72, 73, 75, 76, 77, 78]neutrino mass models to check their consistency with the stringent constraints from cosmology, with various processes like LNV, LFV etc. We have taken the leading order mass matrices obeying μ-τ symmetry originating from type I (II) seesaw then incorporating type II (I) seesaw as perturbations to generate non-zero θ_{13}. Then we studied the LFV in the LRSM framework and further correlated the LFV of the processes ($\mu \to e\gamma$) and ($\mu \to 3$e) with lightest neutrino mass and atmospheric mixing angle, θ_{23} in different neutrino mass models favoring $\mu-\tau$ symmetry. In NDBD, we discuss the different contributions [64] from RH neutrinos and RH gauge bosons, triplet Higgs [66] as well as light-heavy neutrino mixing that can contribute to the effective mass governing the process and identify the significant ones. In this work, we have considered only the dominant new physics contribution as coming from the diagrams containing purely RH current mediated by the heavy gauge boson, $\mathrm{W_R}$ by the exchange of heavy RH neutrino, $\mathrm{N_R}$ and another from the charged Higgs scalar Δ_R mediated by the heavy gauge boson $\mathrm{W_R}$ [65]. We have ignored the contributions coming from the left-right gauge boson mixing and heavy light neutrino mixing.

This chapter is structured as follows. In section 2.2 we very briefly review the left-right symmetric model and the origin of neutrino mass and summarize the NDBD process in this framework in section 2.3. We also discuss the different Feynman diagrams contributing to the amplitude of the decay process (the new physics contribution) in this section. In section 2.4, we briefly discuss lepton flavor violating processes, mainly ($\mu \to 3$e) and ($\mu \to \mathrm{e}\gamma$). We present our numerical analysis and results in section 2.5 and then in section 2.6, we conclude by giving a brief overview of our work.

2.2 Left-right symmetric model and neutrino mass

As has already been discussed in chapter 1, the left-right symmetric model (LRSM) can be considered to be very appealing model for Physics beyond the SM. The seesaw mechanisms can be realized in the context of left-right symmetric model or GUTs where seesaw scale might be related to other physical scales. Herein the gauge group, $\mathrm{SU(3)_c \times SU(2)_L \times SU(2)_R \times U(1)_{B-L}}$ is a very simple extension of the SM gauge group, $\mathrm{SU(3)_c \times SU(2)_L \times U(1)_Y}$. If the Higgs sector of the model is chosen so that RH symmetry is spontaneously broken by triplets, the model gives rise to tiny neutrino masses naturally via seesaw mechanism. Herein, there are 2 sources of lepton number violation, the Majorana masses of neutrinos and Yukawa interaction of triplet Higgs.

We consider the general class of left-right symmetric model with the Higgs content, $\phi(1,2,2,0)$, $\Delta_L(1,2,1,-1)$, $\Delta_R(1,1,2,-1)$. A convenient representation of fields is given by 2× 2 matrices for the Higgs bidoublets and the $\mathrm{SU(2)_{L,R}}$ triplets as,

$$\phi = \begin{bmatrix} \phi_1^0 & \phi_1^+ \\ \phi_2^- & \phi_2^0 \end{bmatrix} \equiv \left(\phi_1, \widetilde{\phi_2}\right), \Delta_{\mathrm{L,R}} = \begin{bmatrix} \delta_{\frac{L,R}{\sqrt{2}}}{}^+ & \delta_{L,R}^{++} \\ \delta_{L,R}^0 & -\delta_{\frac{L,R}{\sqrt{2}}}{}^+. \end{bmatrix} \tag{2.4}$$

The neutral Higgs fields $\delta^0_{\mathrm{L,R}}$, ϕ_1^0, ϕ_2^0 can potentially acquire VEVS $\mathrm{v_R, v_L, k_1, k_2}$ respectively.

$$<\phi>= \begin{bmatrix} \frac{k_1}{\sqrt{2}} & 0 \\ 0 & \frac{k_2}{\sqrt{2}} \end{bmatrix}, <\Delta_{L,R}>= \begin{bmatrix} 0 & 0 \\ \frac{v_{L,R}}{\sqrt{2}} & 0 \end{bmatrix}. \tag{2.5}$$

The VEV $\mathrm{v_R}$ breaks the $\mathrm{SU(2)_R}$ symmetry and sets the mass scale for the extra gauge bosons ($\mathrm{W_R}$ and Z′) and for RH neutrino field (ν_R). The VEVs $\mathrm{k_1}$ and $\mathrm{k_2}$ serves the twin purpose of breaking the remaining the $\mathrm{SU(2)_L \times U(1)_{B-L}}$ symmetry down to $\mathrm{U(1)_{em}}$, thereby setting the mass scales for the observed $\mathrm{W_L}$ and Z bosons and providing Dirac masses for the quarks and leptons. Clearly, $\mathrm{v_R}$ must be significantly larger than $\mathrm{k_1}$ and $\mathrm{k_2}$ in order for $\mathrm{W_R}$ and Z ′ to have greater masses than the W_L and Z bosons. v_L is the VEV of Δ_L, it plays a significant role in the seesaw relation which is the characteristics of the LR model and can be written as,

$$< \Delta_L >= v_L = \frac{\gamma k^2}{v_R} = \frac{\gamma {M_W}^2}{v_R}.. \tag{2.6}$$

The Yukawa lagrangian in the lepton sector is given by,

$$\mathcal{L} = \mathrm{h_{ij}}\overline{\Psi}_{\mathrm{L,i}}\phi\Psi_{\mathrm{R,j}} + \widetilde{\mathrm{h_{ij}}}\overline{\Psi}_{\mathrm{L,i}}\widetilde{\phi}\Psi_{\mathrm{R,j}} + \mathrm{f_{L,ij}}{\Psi_{\mathrm{L,i}}}^{\mathrm{T}}\mathrm{C}i\sigma_2\Delta_{\mathrm{L}}\Psi_{\mathrm{L,j}} + \mathrm{f_{R,ij}}{\Psi_{\mathrm{R,i}}}^{\mathrm{T}}\mathrm{C}i\sigma_2\Delta_{\mathrm{R}}\Psi_{\mathrm{R,j}} + \mathrm{h.c.} \tag{2.7}$$

Where the family indices i, j are summed over, the indices i, j=1, 2, 3 represents the three generations of fermions. $\mathrm{C} = i\gamma_2\gamma_0$ is the charge conjugation operator, $\widetilde{\phi} = \tau_2\phi^*\tau_2$ and γ_μ are the Dirac matrices. Considering discrete parity symmetry, the Majorana Yukawa couplings $f_L = f_R$ (for left-right symmetry) gives rises to Majorana neutrino mass after electroweak symmetry breaking when the triplet Higgs Δ_L and Δ_R acquires non-zero vacuum expectation value. Then equation (6.2) leads to 6×6 neutrino mass matrix as shown in reference 2 of [53],

$$\mathrm{M}_\nu = \begin{bmatrix} M_{LL} & M_D \\ {M_D}^T & M_{RR} \end{bmatrix}, \tag{2.8}$$

where

$$\mathrm{M_D} = \frac{1}{\sqrt{2}}(\mathrm{k_1 h} + \mathrm{k_2}\widetilde{\mathrm{h}}), \mathrm{M_{LL}} = \sqrt{2}\mathrm{v_L f_L}, \mathrm{M_{RR}} = \sqrt{2}\mathrm{v_R f_R}. \tag{2.9}$$

Where M_D, M_{LL} and M_{RR} are the Dirac neutrino mass matrix, LH and RH mass matrix respectively. Assuming $M_L \ll M_D \ll M_R$, the light neutrino mass, generated within a type I+II seesaw can be written as,

$$\mathrm{M}_\nu = {\mathrm{M}_\nu}^{\mathrm{I}} + {\mathrm{M}_\nu}^{\mathrm{II}}, \tag{2.10}$$

$$\mathrm{M}_\nu = \mathrm{M_{LL}} + \mathrm{M_D}{\mathrm{M_{RR}}}^{-1}{\mathrm{M_D}}^{\mathrm{T}} = \sqrt{2}\mathrm{v_L f_L} + \frac{\mathrm{k}^2}{\sqrt{2}\mathrm{v_R}}\mathrm{h_D}{\mathrm{f_R}}^{-1}{\mathrm{h_D}}^{\mathrm{T}}. \tag{2.11}$$

Where the first and second terms in equation (2.11) corresponds to type II seesaw and type I seesaw mediated by RH neutrino respectively. In the context of LRSM both type I and type II seesaw terms can be written in terms of M_{RR} which arises naturally at a high energy scale as a result of spontaneous parity breaking. In LRSM the Majorana Yukawa couplings f_L and f_R are same (i.e., $f_L = f_R$).

Thus equation (2.11) can be written as ,

$$\mathrm{M}_\nu = \gamma \left(\frac{\mathrm{M_W}}{\mathrm{v_R}}\right)^2 \mathrm{M_{RR}} + \mathrm{M_D}\mathrm{M_{RR}}^{-1}\mathrm{M_D}^{\mathrm{T}}. \tag{2.12}$$

Where, γ is a dimensionless parameter defined in (reference [68] [64]).

2.3 $0\nu\beta\beta$ decay in LRSM

NDBD in connection with LRSM has been studied by many theoretical groups[69]. In the context of LRSM, there are several contributions to NDBD in addition to the standard contribution via light Majorana neutrino exchange owing to the presence several heavy additional scalar, vector and fermionic fields. Many of the earlier works have explained it in details with the corresponding Feynman diagrams (see ref. [64]). The different Feynman diagrams corresponding to different contributions to NDBD in LRSM has been shown in chapter 1. The various contributions to $0\nu\beta\beta$ decay transition rate in LRSM are briefly summarized below.

- SM contribution to NDBD where the intermediate particles are the $\mathrm{W_L}^-$ bosons and light neutrinos. The amplitude of this process depends upon the leptonic mixing matrix elements and light neutrino masses.

- Heavy RH neutrino contribution to NDBD in which the mediator particles are the $\mathrm{W_L}^-$ bosons. The amplitude of this process depends upon the mixing between light and heavy neutrinos as well as the mass of the heavy neutrino, $\mathrm{N_i}$.

- Light neutrino contribution to NDBD in which the intermediate particles are $\mathrm{W_R}^-$ bosons. The amplitude of this process depends upon the mixing between light and heavy neutrinos as well as the mass of the RH gauge boson, $\mathrm{W_R}^-$ boson.

- Heavy RH neutrino contribution to NDBD in which the mediator particles are the $\mathrm{W_R}^-$ bosons. The amplitude of this process depends upon the elements of the RH leptonic mixing matrix and the mass of the RH gauge boson, W_R^- boson as well as the mass of the heavy RH Majorana neutrino, N_i.

- Light neutrino contribution from the Feynman diagram mediated by both W_L^- and W_R^-. The amplitude of this process depends upon the mixing between light and heavy neutrinos, leptonic mixing matrix elements, light neutrino masses and the mass of the gauge bosons, W_L^- and W_R^-.

- Heavy neutrino contribution from the Feynman diagram mediated by both W_L^- and W_R^-. The amplitude of the process depends upon the RH leptonic mixing matrix elements, mixing between the light and heavy neutrinos as well as the mass of the gauge bosons, W_L^- and W_R^- and the mass of the heavy RH neutrino, M_i.

- Triplet Higgs Δ_L contribution to NDBD in which the mediator particles are W_L^- bosons. The amplitudes for the process depends upon the masses of the W_L^- bosons, LH triplet Higgs, Δ_L as well as their coupling to leptons, f_L.

- RH triplet Higgs Δ_R contribution to NDBD in which the mediator particles are W_R^- bosons. The amplitude for the process depends upon the masses of the W_R^- bosons, RH triplet Higgs, Δ_R as well as their coupling to leptons, f_R.

However, in this work, we have considered only three of the above-mentioned contributions to NDBD. One from the standard light neutrino contribution through exchange of W_L^- as shown in chapter 1, and the other two are the new physics contributions to NDBD that are mediated by W_R^- and Δ_R respectively. The amplitudes of the contributions are given in several earlier works like [64]. For simple approximations, an assumption of similar mass scales for the heavy particles has been made in the LRSM, where, $M_R \approx M_{W_R} \approx M_{\Delta_L^{++}} \approx M_{\Delta_R^{++}} \approx$ TeV, at a scale accessible at the LHC. Under these assumptions, the amplitude for the light-heavy mixing contribution which is proportional to $\frac{{M_D}^2}{M_R}$ remains very small (since $m_\nu \approx \frac{{M_D}^2}{M_R} \approx (0.01 - 0.1)$eV, $M_D \approx (10^5 - 10^6)$ eV which implies $\frac{M_D}{M_R} \approx (10^{-7} - 10^{-6})$ eV). Thus, we ignore the contributions involving the light and heavy neutrino mixings. For a simplified approach, we have also ignored the mixing between W_L^- and W_R^- bosons owing to the above-mentioned assumptions, which would cause a further suppression in the amplitude of the process (for reference see [65]). Again, the contribution from Δ_L^-, W_L^- is suppressed by the type II seesaw contribution to light neutrino mass and hence neglected here.

Different neutrino mass satisfying the mixing criteria namely, TBM, BM, HM and GRM are considered as a leading contribution in either type I or type II seesaw. The perturbation is added for a generation of non-zero θ_{13} [70] in either of the seesaw terms.

The amplitude of the corresponding processes which we have considered in our work are given by,

- Standard light neutrino contribution,

$$\mathrm{A_{\nu}}^{\mathrm{LL}} \cong \frac{1}{\mathrm{M_{W_L}}^4} \sum \frac{\mathrm{U_{L_{e_i}}}^2 \mathrm{m_i}}{\mathrm{p}^2}. \tag{2.13}$$

  where, $|p| \sim 100$ MeV [71] is the typical momentum transfer at the leptonic vertex, $\mathrm{m_{ee}} = \sum \mathrm{U_{L_{e_i}}}^2 \mathrm{m_i}$ is the effective neutrino mass. $\mathrm{U_{L_{e_i}}}$ represents the elements of the first row of the neutrino mixing matrix, $\mathrm{U_{PMNS}}$.

- Heavy RH neutrino contribution,

$$\mathrm{A_N}^{\mathrm{RR}} \propto \frac{1}{\mathrm{M_{W_L}}^4} \frac{\mathrm{U^*_{R_{e_i}}}^2}{\mathrm{M_i}}. \tag{2.14}$$

- Scalar triplet contribution,

$$\mathrm{A_{\Delta_R}}^{\mathrm{RR}} \propto \frac{1}{\mathrm{M_{W_R}}^4} \frac{1}{\mathrm{M_{\Delta_R}}^2} \mathrm{f_R v_R}. \tag{2.15}$$

  .

Here, $\mathrm{U^*_{R_{e_i}}}$ denotes the first row of the unitary matrix diagonalizing the RH neutrino mass matrix, $\mathrm{M_{RR}}$ with mass eigen values, $\mathrm{M_i}$.

2.4 Lepton Flavor Violation (LFV)

There have been various attempts to observe and predict theoretically the manifestation of LFV involving various modes of muon decay since long. The most promising LFV low energy channels being $\mu \to e\gamma$, $\mu \to 3e$, $\mu \to e$ conversion in nuclei which occur in rates accessible in recent experiments. The selected limits for lepton flavor violating muon decays and muon to electron conversion experiments are shown in table 2.3

DECAY CHANNEL	EXPERIMENT	BRANCHING RATIO LIMIT
$\mu \to e\gamma$	MEG	$< 4.2 \times 10^{-13}$ [72]
$\mu \to 3eeee$	SINDRUM	$< 1.0 \times 10^{-12}$ [73]
$\mu Au \to$ e Au	SINDRUM II	$< 7 \times 10^{-13}$ [74]

Table 2.3: Experimental limits on LFV muon decays.

In the SM seesaw, the LFV decay rates induced by neutrino mixing are suppressed by tiny neutrino masses,$\left(\frac{\Delta m_\nu{}^2}{M_W{}^2}\right) \sim 10^{-50}$ and hence are well below the current experimental limits and even the distant future sensitivities. New physics beyond the SM is required to make the process observable. In LRSM, several new contributions appear due to the additional RH current interactions, which could lead to sizable LFV rates for TeV scale v_R that occur at rates observable in current experiments. LFV in the LRSM has been studied in many previous works. There are various LFV processes providing constraints on the masses of the RH neutrinos and doubly charged scalars. It turns out that the process $\mu \to 3e$ induced by doubly charged bosons Δ_L^{++} and Δ_R^{++} and $\mu \to e\gamma$ provides the most relevant constraint. In this work, we consider these processes in the minimal left-right symmetric model (MLRSM). The limit of branching ratio of the process $\mu \to 3e$ as shown in table 2.3 is $< 1.0 \times 10^{-12}$ at 90% CL was obtained at the Paul Scherrer Institute (PSI) over 20 years ago by the SINDRUM experiment [73]. Presently the Mu3e collaboration has submitted a letter of intent to PSI to perform a new improved search for the decay $\mu \to 3e$ with a sensitivity of 10^{-16} at 95% CL [74] which corresponds to an improvement by four orders of magnitude compared to the former SINDRUM experiment. Whereas the new upper limit for BR of the process $\mu \to e\gamma$ is established to be $< 4.2 \times 10^{-13}$ at 90% CL by the MEG collaboration. Taking into account the contributions from heavy RH neutrinos and Higgs scalars, the expected branching ratios and conversion rates of the above processes have been calculated in the LRSM in the work [75]. The corresponding BR for the process ($\mu \to 3e$) as defined in chapter 1 is given by,

$$\mathrm{BR}\,(\mu \to 3\mathrm{e}) = \frac{1}{2}|\mathrm{h}_{\mu\mathrm{e}}\mathrm{h}_{\mathrm{ee}}^*|^2 \left(\frac{\mathrm{m_{W_L}}^4}{\mathrm{M}_{\Delta_\mathrm{L}}^{++4}} + \frac{\mathrm{m_{W_R}}^4}{\mathrm{M}_{\Delta_\mathrm{R}}^{++4}}\right). \tag{2.16}$$

Where h_{ij} describes the lepton Higgs coupling in LRSM and is given by equation (1.106). For the process ($\mu \to e\gamma$), however we have not considered all the possible contributions, the relevant BR we used is given by,

$$\mathrm{BR}\left(\mu \rightarrow \mathrm{e}\gamma\right) = 1.5 \times 10^{-7}|\mathrm{g_{lfv}}|^2\left(\frac{1\mathrm{TeV}}{\mathrm{M_{W_R}}}\right)^4, \tag{2.17}$$

where, g_{lfv} is defined as,

$$\mathrm{g_{lfv}} = \sum_{\mathrm{n=1}}^{3} \mathrm{V}_{\mu\mathrm{n}}\mathrm{V_{en}}^*\left(\frac{\mathrm{M_n}}{\mathrm{M_{W_R}}}\right)^2 = \frac{[\mathrm{M_R M_R}^*]_{\mu\mathrm{e}}}{\mathrm{M_{W_R}}^2} \tag{2.18}$$

The sum is over the heavy neutrinos only. $\mathrm{M}^{++}_{\Delta_{\mathrm{L,R}}}$ are the masses of the doubly charged bosons, $\Delta_{\mathrm{L,R}}{}^{++}$, V is the mixing matrix of the RH neutrinos with the electrons and muons. $\mathrm{M_n}(\mathrm{n} = 1, 2, 3)$ are the RH neutrino masses.

2.5 Numerical analysis and results

In our present work, we have studied LNV (NDBD) for standard as well as non-standard contributions for the effective mass as well as the half-life governing the decay process in the framework of LRSM. We have also correlated the LFV of the process, $\mu \rightarrow 3\mathrm{e}$ and $\mu \rightarrow \mathrm{e}\gamma$ with the lightest neutrino mass and atmospheric mixing angle, θ_{23} respectively for both normal and inverted mass hierarchies. In this section, we present a detailed analysis of our work and we have divided it into different subsections, firstly the standard light neutrino contribution to NDBD and then the new physics contribution to NDBD considering perturbation in type II and then type I seesaw. Lastly, we have shown the analysis of correlating LFV with $\mathrm{m_{lightest}}$ and θ_{23}.

2.5.1 Standard light neutrino contribution

For NDBD mediated by the light Majorana neutrinos, the half-life of the decay process is given by equation (2.1) and the effective mass governing the process is as given in equation (2.2). In our present work, we first evaluated the effective light neutrino mass within the standard mechanism using the formula (2.1) where, $\mathrm{U_{ej}}$ are the elements of the first row of the neutrino mixing matrix, U (dependent on the known parameters θ_{13}, θ_{12} and the unknown Majorana phases α and β). $\mathrm{U_{PMNS}}$ is the diagonalizing matrix of the light neutrino mass matrix, m_ν, such that,

$$\mathrm{m}_\nu = \mathrm{U_{PMNS}} \mathrm{M}_\nu{}^{(\mathrm{diag})} \mathrm{U_{PMNS}}{}^{\mathrm{T}}, \tag{2.19}$$

where $\mathrm{M}_\nu{}^{(\mathrm{diag})} = \mathrm{diag}(\mathrm{m}_1, \mathrm{m}_2, \mathrm{m}_3)$. In the case of 3 neutrino mixing, 2 ν mass spectra are possible,

- Normal Hierachy (NH) which corresponds to $m_1 < m_2 \ll m_3$; $\Delta m_{12}{}^2 \ll \Delta m_{23}{}^2$.
- Inverted Hierarchy (IH) which corresponds to $m_3 \ll m_1 \sim m_2$; $\Delta m_{12}{}^2 \ll |\Delta m_{13}{}^2|$.

In both the spectra, $\Delta \mathrm{m}_{12}{}^2 = \Delta \mathrm{m}_{\mathrm{solar}}{}^2$. For NH, $\Delta \mathrm{m}_{23}{}^2 = \Delta \mathrm{m}_{\mathrm{atm}}{}^2$ and for IH, $|\Delta m_{13}{}^2| = \Delta m_{atm}{}^2$. In the case of NH, the neutrino masses m_2 and m_3 are connected with the lightest mass m_1 by the relation,

$$\mathrm{m}_2 = \sqrt{\mathrm{m}_1^2 + \Delta \mathrm{m}_{\mathrm{sol}}^2}, \mathrm{m}_3 = \sqrt{\mathrm{m}_1^2 + \Delta \mathrm{m}_{\mathrm{sol}}^2 + \Delta \mathrm{m}_{\mathrm{atm}}^2}. \tag{2.20}$$

In IH, m_3 is the lightest mass and we have,

$$\mathrm{m}_1 = \sqrt{\mathrm{m}_3^2 + \Delta \mathrm{m}_{\mathrm{atm}}^2}, \mathrm{m}_2 = \sqrt{\mathrm{m}_3^2 + \Delta \mathrm{m}_{\mathrm{sol}}^2 + \Delta \mathrm{m}_{\mathrm{atm}}^2}. \tag{2.21}$$

For both the normal and inverted hierarchies, equation (2.6) can be written in terms of lightest neutrino mass as,

for NH,

$$\mathrm{m}_{\beta\beta} = \mathrm{m}_1 \mathrm{c}_{12}{}^2 \mathrm{c}_{13}{}^2 + \sqrt{(\mathrm{m}_1^2 + \Delta \mathrm{m}_{\mathrm{sol}}^2} \mathrm{s}_{12}{}^2 \mathrm{c}_{13}{}^2 \mathrm{e}^{2\mathrm{i}\alpha}) + \sqrt{(\mathrm{m}_1^2 + \Delta \mathrm{m}_{\mathrm{sol}}^2 + \Delta \mathrm{m}_{\mathrm{atm}}^2} \mathrm{s}_{13}{}^2 \mathrm{e}^{2\mathrm{i}\beta}), \tag{2.22}$$

for IH,

$$\mathrm{m}_{\beta\beta} = \sqrt{(\mathrm{m}_3^2 + \Delta \mathrm{m}_{\mathrm{atm}}^2} \mathrm{c}_{12}{}^2 \mathrm{c}_{13}{}^2) + \sqrt{(\mathrm{m}_3^2 + \Delta \mathrm{m}_{\mathrm{sol}}^2 + \Delta \mathrm{m}_{\mathrm{atm}}^2} \mathrm{s}_{12}{}^2 \mathrm{c}_{13}{}^2 \mathrm{e}^{2\mathrm{i}\alpha} + \mathrm{m}_3 \mathrm{s}_{13}{}^2 \mathrm{e}^{2\mathrm{i}\beta}). \tag{2.23}$$

The 3σ ranges of the mass squared differences and mixing angles from global analysis of oscillation data are outlined as in table 2.1. Using the best fit values of the mass squared differences and the 3σ ranges of the three mixing angles from a global analysis of oscillation data (as shown in table 2.1, we have shown the variation of the effective Majorana mass as a function of the lightest neutrino mass m_1 (for NH) and m_3 (for IH). During our calculation, we have varied the Majorana phase α and β from 0 to 2π. The effective mass assumes different values depending on whether the neutrino mass states follows normal hierarchy

(NH) or inverted hierarchy (IH). We have used equations (2.22) and (2.23) in evaluating the effective mass in terms of the lightest neutrino mass. The variation is shown in figure (2.1). It is seen from the figure that the light neutrino contribution to neutrinoless double beta decay ($0\nu\beta\beta$) can saturate the bound imposed by KamLAND-Zen ($\leq 0.061 - 0.165$eV) [reference ([37])] only for the higher values of lightest neutrino masses which is disallowed by the Planck data (lightest mass for NH ~ 0.07 and lightest mass for IH ~ 0.065).

Again, we have evaluated the effective majorana mass for different leptonic mixing patterns possessing $\mu - \tau$ symmetry, namely, tribimaximal, golden ratio and hexagonal mixing using equation (2.22)and (2.23). In all the different $\mu - \tau$ symmetric mixing patterns which we have considered, i.e., TBM, HM, GRM, the reactor mixing angle θ_{13} is 0 and θ_{23} is 45^0. Whereas θ_{12}=35.5^0, (for TBM), $\theta_{12} = 30^0$ (for HM), θ_{12}=31.71^0 (for GRM). Since, θ_{12}=45^0, i.e., BM has been ruled out by experiments, we have ignored this case for the standard contributions. Again, it is to be noted that there are two values of θ_{12} for GRM, which are, 31.7^0 and 35.96^0 [45]. In this study, we have considered the first value which is allowed as mentioned in reference [45][46, 47]

The variations of m_ν^{eff} for the different mixing patterns for NH and IH in terms of lightest neutrino mass are shown as in figure (2.2).

2.5.2 New physics contribution to NDBD considering perturbation in type II seesaw.

For the new Physics contribution, we have considered the contributions of $0\nu\beta\beta$ from the RH current and from the triplet Higgs (Δ_R). The contributions from the LH Higgs triplet, Δ_L is suppressed by the light neutrino mass. Also, we consider the mixing between LH and RH sector to be so small that their contributions to $0\nu\beta\beta$ can be neglected. The total effective mass is thus given by the formula, (as in [65])

$$m_{N+\Delta_R}{}^{eff} = p^2 \frac{{M_{W_L}}^4}{{M_{W_R}}^4} \frac{{U_{Rei}}^{*2}}{M_i} + p^2 \frac{{M_{W_L}}^4}{{M_{W_R}}^4} \frac{{U_{Rei}}^2 M_i}{{M_{\Delta_R}}^2}. \tag{2.24}$$

Here, $< p^2 >= m_e m_p \frac{M_N}{M_\nu}$ is the typical momentum exchange of the process, where m_p and m_e are the mass of the proton and electron respectively and M_N is the NME corresponding to the RH neutrino exchange. We know that TeV scale LRSM plays an important role in

$0\nu\beta\beta$ decay. We have considered the values $\mathrm{M_{W_R}} = 3.5$ TeV, $\mathrm{M_{W_L}} = 80$ GeV, $\mathrm{M_{\Delta_R}} \approx 3$ TeV, the heavy RH neutrino $\approx$ TeV which are within the recent collider limits [76]. The allowed value of p (the virtuality of the exchanged neutrino) is in the range $\sim$ (100-200) MeV. In our analysis, we have taken p$\simeq$180 MeV [64].

Thus,

$$\mathrm{p}^2 \frac{\mathrm{M_{W_L}}^4}{\mathrm{M_{W_R}}^4} \simeq 10^{10}\mathrm{eV}^2. \tag{2.25}$$

However, equation (2.24) is valid only in the limit $\mathrm{M_i}^2 \gg |<\mathrm{p}^2>|$ and $\mathrm{M_\Delta}^2 \gg |<\mathrm{p}^2>|$. The formula for light ν masses in LRSM can be written as,

$$\mathrm{M}_\nu = \mathrm{M}_\nu{}^{\mathrm{I}} + \mathrm{M}_\nu{}^{\mathrm{II}}, \tag{2.26}$$

$$\mathrm{U_{PMNS}}\mathrm{M}_\nu{}^{(\mathrm{diag})}\mathrm{U_{PMNS}}{}^{\mathrm{T}} = \mathrm{M}_\nu{}^{\mathrm{II}} + \mathrm{U}_{(\mu-\tau)}\mathrm{U_{Maj}}\mathrm{M}_\nu{}^{\mathrm{I(diag)}}\mathrm{U_{Maj}}{}^{\mathrm{T}}\mathrm{U}_{(\mu-\tau)}{}^{\mathrm{T}}, \tag{2.27}$$

where, $\mathrm{U_{PMNS}}$ and $U_{(\mu-\tau)}$ represents the diagonalizing matrix of M_ν and $\mathrm{M}_\nu{}^{\mathrm{I}}$. The Majorana phases have been taken in the type I seesaw term [65]. From equation (2.26) we can evaluate $\mathrm{M}_\nu{}^{\mathrm{II}}$. We have considered the case when $\mathrm{M}_\nu{}^{\mathrm{I}}$ possess $\mu-\tau$ symmetry, with the various choices for mixing matrices such as TBM, BM, HM, GRM, with uniquely predicting $\theta_{13} = 0$. We have considered $\mathrm{M}_\nu{}^{\mathrm{I(diag)}} = \mathrm{X}\mathrm{M}_\nu{}^{(\mathrm{diag})}$, where we have introduced the parameter X to describe the relative strength of the type I and II seesaw terms. The parameter X can take any numerical value provided the two seesaw terms gives rise to correct light neutrino mass matrix. In our case, we have considered X=0.5, i.e., equal contributions from both the seesaw terms. The required correction to $\mu-\tau$ type ν mass matrix for generation of non-zero reactor mixing angle (θ_{13}) can be obtained from the perturbation matrix, $\mathrm{M}_\nu{}^{\mathrm{II}}$ mass matrix. $\mathrm{M}_\nu{}^{\mathrm{II}}$ can be constructed as,

$$\mathrm{M}_\nu{}^{\mathrm{II}} = \begin{bmatrix} S_{11} & S_{12} & S_{13} \\ S_{21} & S_{22} & S_{23} \\ S_{31} & S_{32} & S_{33} \end{bmatrix}. \tag{2.28}$$

It can be derived using equation (2.27). The type II seesaw mass matrix is evaluated in terms of light neutrino mass matrix, constructed using the best-fit neutrino data and $\mu-\tau$ symmetric type I mass matrices (TBM, BM, HM, GRM). The elements are shown in the appendix A.1.

To evaluate $m_{N+\Delta_R}{}^{eff}$, we need the diagonalizing matrix of the heavy RH Majorana mass matrix M_{RR}, U_{Rei} and its mass eigenvalues, M_i. M_{RR} can be written in the form(from reference [77]) and is evident from equation (2.12),

$$M_{RR} = \frac{1}{\gamma}\left(\frac{v_R}{M_{W_L}}\right)^2 {M_\nu}^{II}, \tag{2.29}$$

$${M_\nu}^{II} = U_{PMNS}{M_\nu}^{(diag)}{U_{PMNS}}^T - U_{(\mu-\tau)}U_{Maj}{M_\nu}^{I(diag)}{U_{Maj}}^T{U_{(\mu-\tau)}}^T. \tag{2.30}$$

In the above equation, $U_{(\mu-\tau)}$ represents U_{TBM}, U_{BM}, U_{HM}, U_{GRM} , i.e., the diagonalizing matrices of the TBM, BM, HM and GRM mass matrices. For TeV scale type I + type II seesaw, we have fine tuned the dimensionless parameter, $\gamma \sim 10^{-10}$, we have considered $v_R \sim TeV$. Thus after obtaining M_{RR}, we diagonalized it and obtained the eigenvalues, M_i and its diagonalizing matrix in terms of the lightest neutrino mass (m_1 or m_3)for (NH/IH) and the Majorana phases (α and β). We have varied the Majorana phases α and β from 0 to 2π and evaluated the effective mass for new physics contribution using formula (2.24) in terms of lightest neutrino mass. This is shown in figure 2.3. We have imposed the KamLAND-Zen bound on the new physics contribution to effective mass and the Planck bound on the sum of the absolute neutrino mass.

2.5.3 New physics contribution to NDBD considering perturbation in type I seesaw.

Alternatively, we have again considered the type II seesaw to give rise to $\mu-\tau$ type neutrino mass matrix and the necessary correction to obtain non-zero θ_{13} is obtained from the type I seesaw term. Thus, ${M_\nu}^{II}$ in equation (2.27) can be written as,

$${M_\nu}^{II} = U_{(\mu-\tau)}U_{Maj}{M_\nu}^{II(diag)}{U_{Maj}}^T{U_{(\mu-\tau)}}^T, \tag{2.31}$$

where, $U_{(\mu-\tau)}$ represents $U_{TBM}, U_{BM}, U_{HM}, U_{GRM}$.

$${M_\nu}^{I} = M_\nu - {M_\nu}^{II}, \tag{2.32}$$

$${M_\nu}^{I} = U_{PMNS}{M_\nu}^{(diag)}{U_{PMNS}}^T - {M_\nu}^{II}. \tag{2.33}$$

Like in the previous case, we have again evaluated the RH Majorana mass matrix using equation (2.29). We have fine tuned the dimensionless parameter γ and then by diagonalizing the RH Majorana mass matrix M_{RR}, we have obtained U_{Rei} and the eigenvalues, M_i

(i.e., $\mathrm{M_{RR}}^{(\mathrm{diag})}$) where,

$$\mathrm{M_{RR}} = \mathrm{U_{Rei}} \mathrm{M_{RR}}^{(\mathrm{diag})} \mathrm{U_{Rei}}^{\mathrm{T}} \tag{2.34}$$

We then evaluated the effective Majorana mass, $\mathrm{m_{N+\Delta_R}}^{\mathrm{eff}}$ using equation (2.24) as a function of the lightest LH neutrino mass. This is shown in figure 2.4. When we consider the type II seesaw term to be $\mu - \tau$ symmetric and the perturbation from the type I seesaw term, the type I seesaw mass matrix can be derived as in the previous case and is shown in the appendix A.1. For the new physics contribution in which the type II term acts as the perturbation, we have also evaluated the half-life of the $0\nu\beta\beta$ decay process using equation (2.1), where,

$$\left|\mathrm{m}_{\nu}{}^{\mathrm{eff}}\right|^2 = \left|\mathrm{m_N}^{\mathrm{eff}} + \mathrm{m}_{\Delta_\mathrm{R}}{}^{\mathrm{eff}}\right|^2. \tag{2.35}$$

By substituting the values of the phase factors($G_0{}^{\nu}$) [78] [79], nuclear matrix element(NME) [80] [79] and mass of electron, we have obtained the half-life as a function of the lightest mass in the different mixing patterns for both NH and IH, as shown in figure 2.5. In a similar process, we have also computed the half-life for new physics contribution to NDBD in which the type I term acts as the perturbation, for a generation of non-zero θ_{13}. It is shown in figure 2.6.

2.5.4 Correlating LFV with lightest neutrino mass and θ_{23}

To correlate LFV with neutrino mass in our analysis, we have considered the LFV processes, $\mu \to 3\mathrm{e}$ and $\mu \to \mathrm{e}\gamma$. The BR for both the processes have a strong flavor dependence on the RH mixing matrix. Since the process $\mu \to 3\mathrm{e}$ is controlled by $\mathrm{h}_{\mu\mathrm{e}}\mathrm{h}^*_{\mathrm{ee}}$ whereas $\mu \to \mathrm{e}\gamma$ is controlled by the factor $[\mathrm{M_R M_R}^*]_{\mu\mathrm{e}}$, the later is independent of the Majorana CP phases and the lightest neutrino mass, $\mathrm{m_j}$. We have correlated the BR of the process $\mu \to 3\mathrm{e}$ with the lightest neutrino mass ($\mathrm{m_1/m_3}$) for (NH/IH). The BR of the process $\mu \to \mathrm{e}\gamma$ is correlated with the atmospheric mixing angle, θ_{23}, since the other two mixing angles θ_{12} and θ_{13} are measured precisely. For calculating the BR, we used the expression given in equation (2.16) and (2.17). The lepton Higgs coupling $\mathrm{h_{ij}}$ in (2.17) can be computed explicitly for a given RH neutrino mass matrix by diagonalizing the RH neutrino mass matrix and obtaining the mixing matrix element, V_i and the eigenvalues M_i. For evaluating M_{RR}, we need to know $\mathrm{M}_{\nu}{}^{\mathrm{II}}$, as evident from equation (2.29). We computed $M_{\nu}{}^{II}$ from equation (2.31). For determining the BR for $\mu \to 3e$, we imposed the best fit values of the parameters, $\Delta m_{sol}{}^2$, $\Delta m_{atm}{}^2$, δ, θ_{13}, θ_{23}, θ_{12} in M_ν. The numerical values of $M_\nu{}^I$ can be computed as before for different mixing patterns, TBM, BM, HM, GRM. Thus, we get $M_\nu{}^{II}$ as a function of the parameters α, β and $m_{lightest}$. Then varying both the Majorana phases, α, β from 0 to 2π, we obtained $M_\nu{}^{II}$ as a function of $m_{lightest}$. Similarly, for $\mu \to e\gamma$ we substituted the values of the lightest mass (m1/m3) for (NH/IH) as (0.07eV/0.065eV) and best fit values for the parameters $\Delta m_{sol}{}^2$, $\Delta m_{atm}{}^2$, δ, θ_{13}, while varying both the Majorana phases, α, β from 0 to 2π and thus obtained $M_\nu{}^{II}$ and hence M_{RR} as a function of the atmospheric mixing angle θ_{23}. Thus BR can be obtained as a function of $\sin^2\theta_{23}$ from equation (2.17). We have varied the value of $\sin^2\theta_{23}$ in its 3σ range as in table 2.1 and the lightest neutrino mass from 10^{-3} to 10^{-1} and obtained the values of BR for different mixing patterns, TBM, BM, HM, GRM. The variation is shown in figures 2.7, 2.8, 2.9 and 2.10 for both NH and IH.

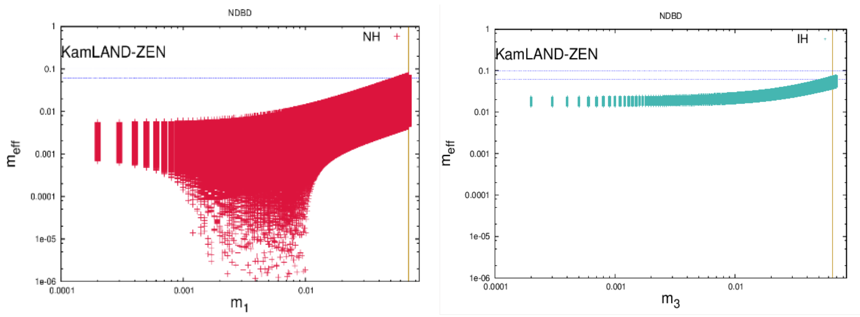

Figure 2.1: Effective Majorana mass for $0\nu\beta\beta$ as a function of lightest neutrino mass, m_1 (in eV) for NH (fig. left) and m_3 (in eV) for IH (fig. right) within the standard mechanism. The blue dashed line and the yellow solid line represents the KamLAND-Zen bound on the effective mass and the Planck bound on the sum of the absolute neutrino mass respectively.

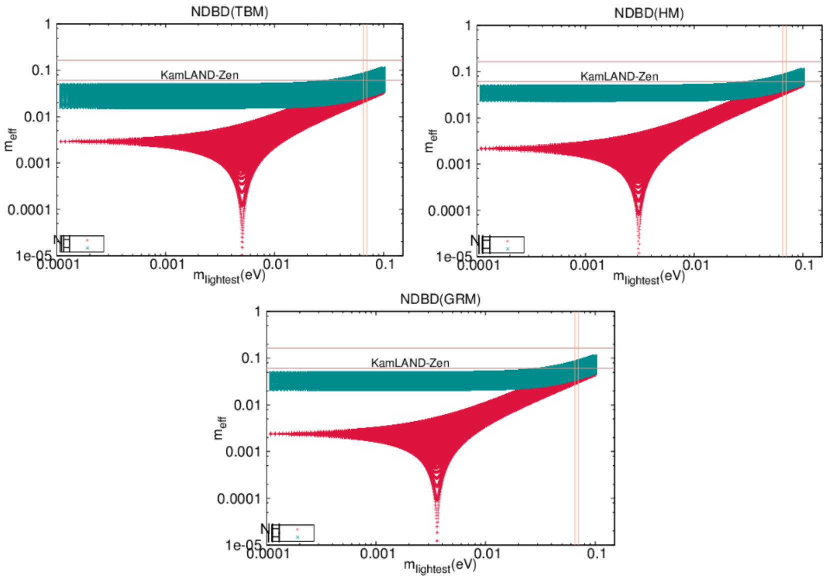

Figure 2.2: Standard light neutrino contribution to eff. mass for $0\nu\beta\beta$ for TBM, HM and GRM mixing patterns as a function of lightest neutrino mass (in eV) for NH/IH (m1/m3). The horizontal lines represents the upper limit of effective mass propounded by kamLAND-Zen and vertical line represents the Planck bound on lightest neutrino mass for NH/IH.

.

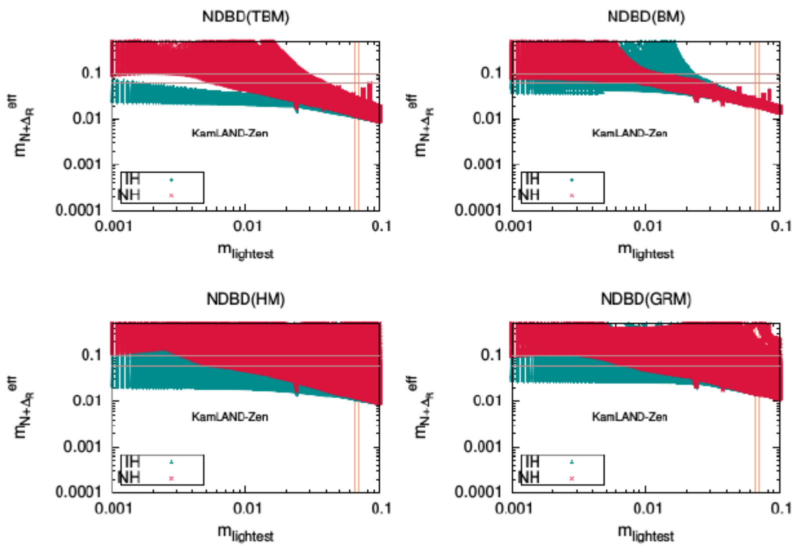

Figure 2.3: New Physics contribution to effective mass for $0\nu\beta\beta$ considering perturbation in type II seesaw for different mass models (TBM, BM, HM and GRM).

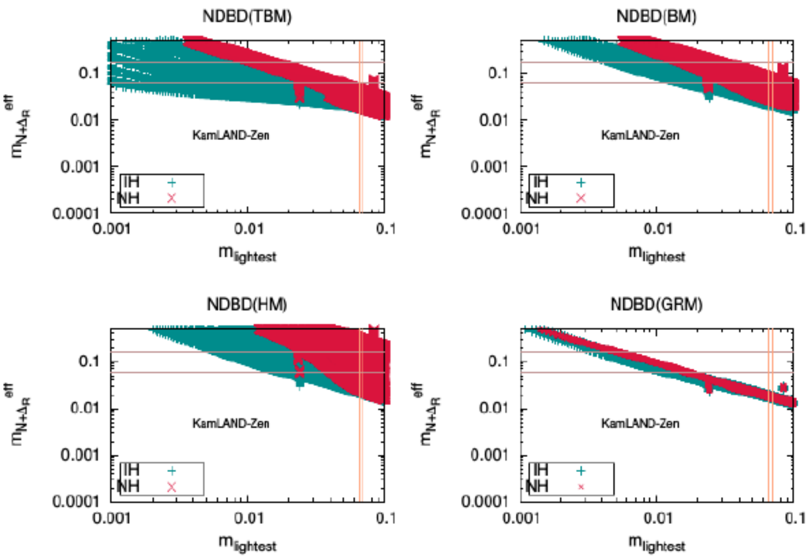

Figure 2.4: New Physics contribution to effective mass for $0\nu\beta\beta$ considering perturbation in type I seesaw for different mass models (TBM, BM, HM and GRM).

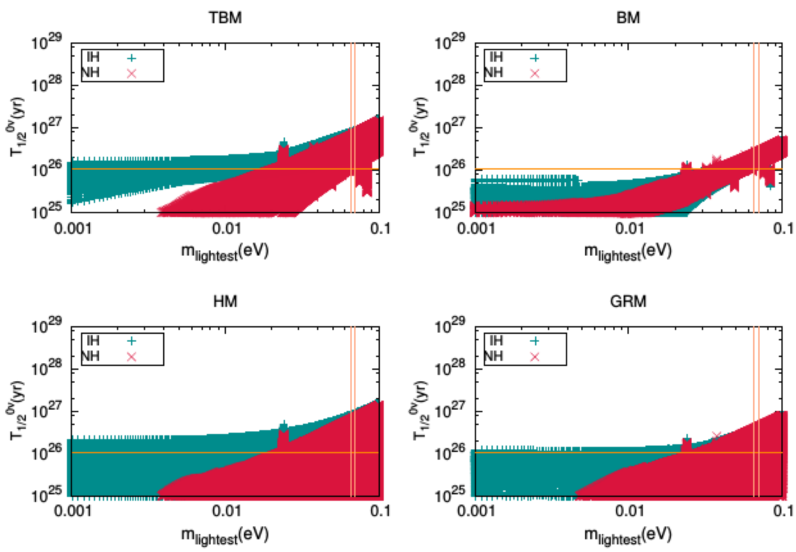

Figure 2.5: New Physics contributions to half-life of $0\nu\beta\beta$ considering perturbation in type II seesaw in different mass models (TBM, BM, GRM, HM) for normal and inverted hierarchies. The horizontal line represents the lower limit on $0\nu\beta\beta$ half-life imposed by KamLAND-ZEN projected sensitivity respectively.

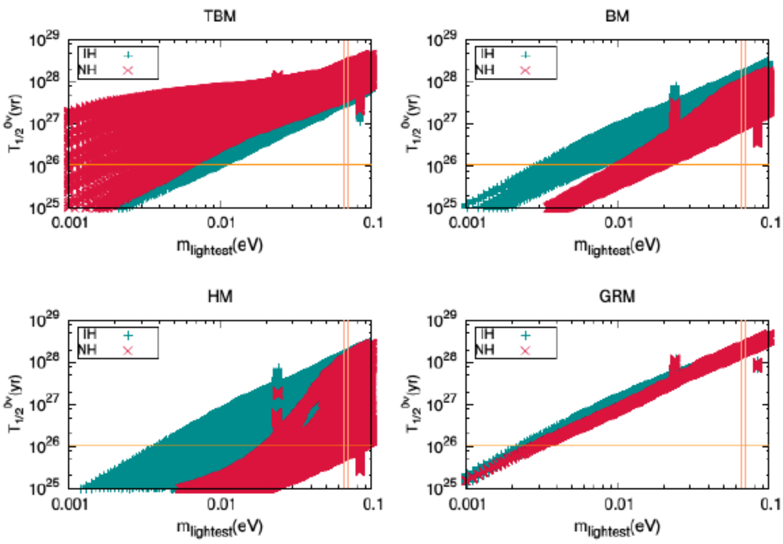

Figure 2.6: New Physics contributions to half-life of $0\nu\beta\beta$ considering perturbation in type I seesaw in different mass models (TBM, BM, GRM, HM) for normal and inverted hierarchies. The horizontal line represents the lower limit on $0\nu\beta\beta$ half-life imposed by KamLAND-ZEN projected sensitivity respectively.

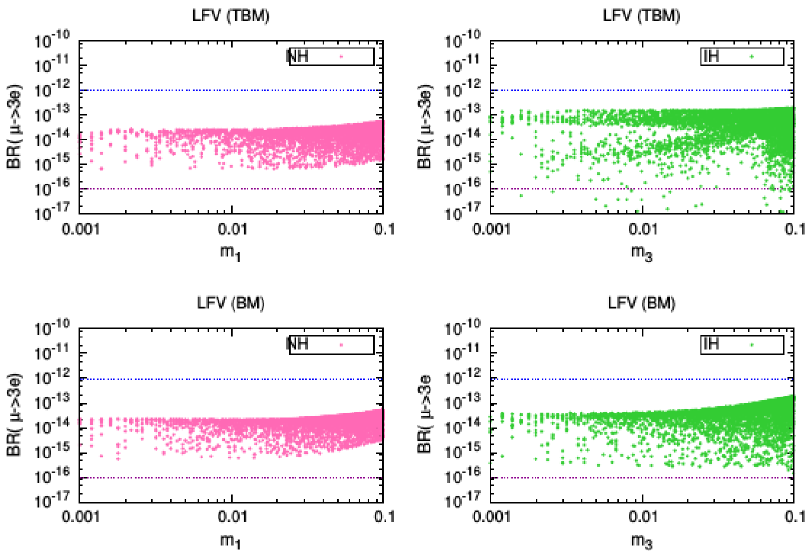

Figure 2.7: Total contribution to lepton flavor violation shown as a function of the lightest neutrino mass for the TBM and BM neutrino mass models for normal and inverted hierarchies. The blue and violet dashed line shows the limit of BR as given by SINDRUM experiment and the recently proposed limit of μ 3e experiment respectively.

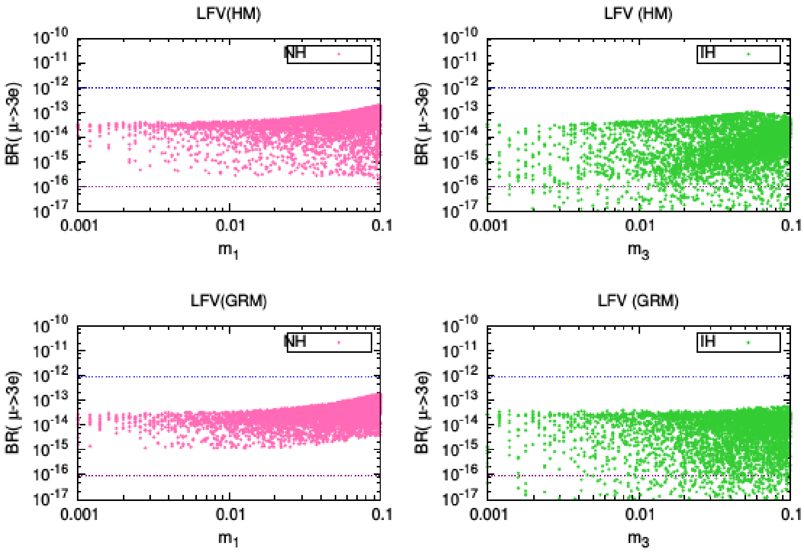

Figure 2.8: Total contribution to lepton flavor violation with type (I+II) seesaw shown as a function of the lightest neutrino mass for the HM and GRM neutrino mass models for normal and inverted hierarchies. The blue and violet dashed line shows the limit of BR as given by SINDRUM experiment and the recently proposed limit of μ 3e experiment respectively.

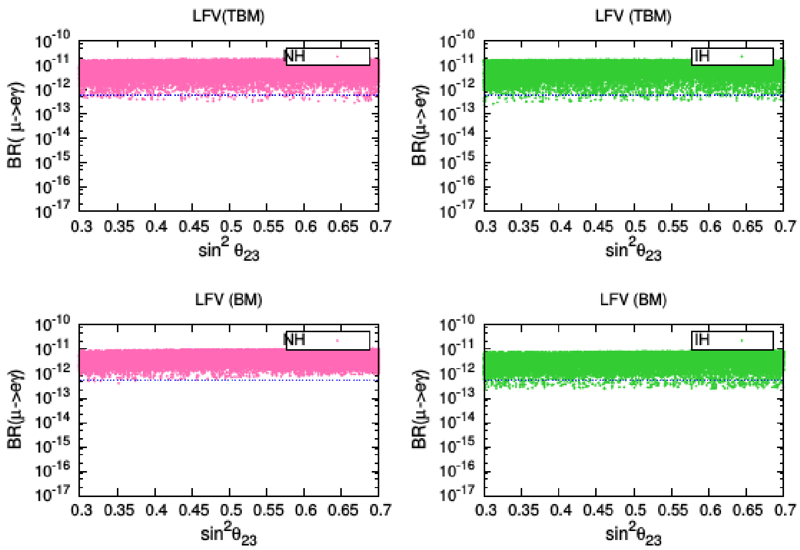

Figure 2.9: Total contribution to lepton flavor violation with type (I+II) seesaw shown as a function of the atmospheric mixing angle θ_{23} for TBM and BM neutrino mass models for normal and inverted hierarchies. The blue dashed line shows the limit of BR.

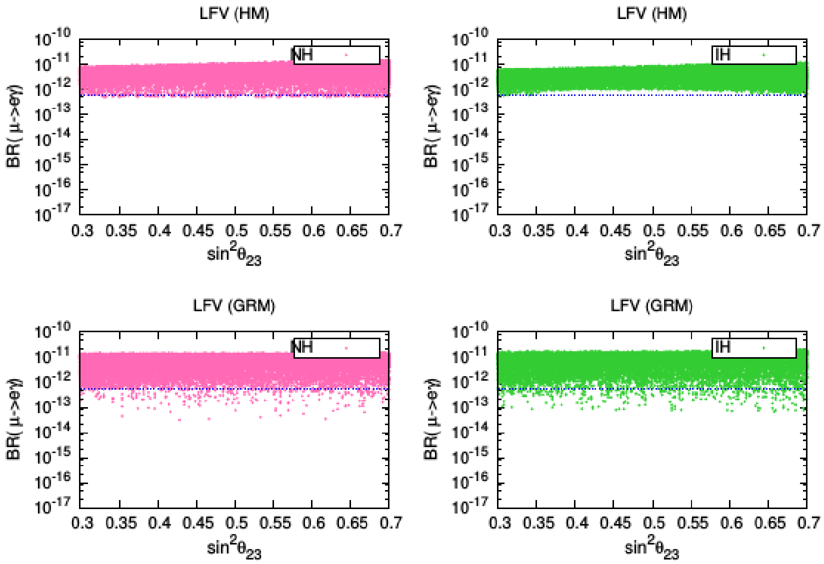

Figure 2.10: Total contribution to lepton flavor violation with type (I+II) seesaw shown as a function of the atmospheric mixing angle θ_{23} for HM and GRM neutrino mass models for normal and inverted hierarchies. The blue dashed line shows the limit of BR.

2.6 Conclusion

In this chapter, we contemplated the implications of NDBD and LFV in LRSM framework. Owing to the presence of new scalars and gauge bosons in this model, various additional sources would give rise to contributions to NDBD process, which involves RH neutrinos, RH gauge bosons, scalar Higgs triplets as well as the mixed LH-RH contributions. For a simplified analysis, we have ignored the left-right gauge boson mixing and heavy light neutrino mixing. We have considered the extra gauge bosons and scalars to be of the order of TeV. Again, the existence of non-zero θ_{13} has many implications in the neutrino sector beyond SM. A simple way to accommodate non-zero θ_{13} is by adding a perturbation matrix to the neutrino mass matrix. A well known neutrino mass mixing pattern is the one obeying $\mu-\tau$ symmetry. In our present analysis, we have considered the different realizations of the $\mu-\tau$ symmetric mass matrices, namely, TBM, BM, HM and GRM. The perturbation to this matrices to generate non-zero θ_{13} is obtained from either of the seesaw terms, type I and type II. We have considered two different approaches, type I giving $\mu-\tau$ symmetry and type II as a perturbation, type II giving $\mu-\tau$ symmetry and type I as a perturbation, for generation of a non-zero θ_{13}. We analyzed the standard as well as new physics contribution to the effective mass m_{eff} governing NDBD as well as the half-life considering both type I and type II seesaw. We have shown the variations of the effective mass as well as the half-life with the lightest neutrino mass which corresponds to the standard as well as the non-standard contributions. We have seen from our analysis that both the approaches yield different consequences in NDBD. The various parameters we have chosen for our numerical analysis are consistent with constraints from ν oscillation experiments. We have also discussed the impacts of the lightest neutrino mass and not so precisely known atmospheric mixing angle, θ_{23} on the behaviour of LFV of the decay process, $\mu \rightarrow 3e$ and $\mu \rightarrow e\gamma$ respectively. Based on our observations, the following conclusions could be arrived at,

- In the standard light neutrino contribution to NDBD, it is observed that all the mass patterns (TBM, HM, GRM) yield almost similar results for NH mass spectrum. The effective mass governing NDBD is found to be of the order of 10^{-3} eV and are within and much below the current experimental limit [37]. Whereas in case of IH mass spectrum, for TBM, HM and GRM, the values of effective mass are found to be within and close to the experimental limit and are of the order of 10^{-2} eV. However, in all the cases, the light neutrino contribution can saturate the experimental limit for lightest neutrino mass (m_1/m_3) for (NH/IH) of around 0.1 eV.

- In new physics contribution considering perturbation in type II seesaw, for IH, TBM, HM and GRM shows results within the recent experimental bound for lightest mass varying from (0.001-0.1) eV. Whereas, for NH the effective mass lies within the experimental limit for lightest mass in the range (0.01-0.1) eV. In case of half-life also, except BM mass pattern, TBM, HM and GRM schemes show better results. In all the cases, both NH and IH seems to be more compatible with the experimental results.

- In new physics contribution considering perturbation in type I seesaw, the values that are consistent with experimental bound imposed by KamLAND-Zen are found for lightest mass (0.001-0.1) eV for TBM and about (0.01-0.1 eV) for all other cases. Whereas for half-life, TBM shows better results. In all other mixing patterns, half-life lies within experimental bound for values of lightest mass lying from (0.005-0.1) eV for IH.

- It is observed from our analysis that the BR for the process $\mu \rightarrow 3e$ in the LRSM remains consistent with the experimental bound for a wide range of light neutrino mass. However, it depends on the neutrino mass spectrum as evident from fig. 2.7 and 2.8. In case of IH, the BR is spread over a wide range and lies even in the range of the recently proposed limit with a sensitivity of 10^{-16}. For the process, $\mu \rightarrow e\gamma$, the results for BR are found to be consistent with the experimental limit for all the mixing patterns, except for HM and BM (NH) in the 3σ range of θ_{23}. In this case, the dependence of LFV on the neutrino mass spectrum is not much significant as seen in fig. 2.9 and 2.10.

The effective neutrino mass depends on the nature of the neutrino mass spectrum. In most of our analysis in case of NDBD as well as LFV, we have observed that both the hierarchical patterns shows almost equal dominance. However, it is easier to observe the process if we consider the leading order mass matrices obeying μ-τ symmetry originating from type I seesaw and using type II seesaw as perturbations to generate non-zero θ_{13}. Nevertheless, a more detailed analysis considering the presence of all the mechanisms which can generate the process in the LRSM framework should be pursued to give a general conclusion.

Bibliography

[1] Fukuda, S., et al. Constraints on neutrino oscillations using 1258 days of Super-Kamiokande solar neutrino data. *Phys. Rev. Lett.*, 86:5656, 2001.

[2] Ahmad, Q. R., et al. Direct evidence for neutrino flavor transformation from neutral current interactions in the Sudbury Neutrino Observatory. *Phys. Rev. Lett.*, 89:011301, 2002.

[3] Ahmad, Q. R., et al. Measurement of day and night neutrino energy spectra at SNO and constraints on neutrino mixing parameters. *Phys. Rev. Lett.*, 89:011302, 2002.

[4] Abe, S., et al. Precision Measurement of Neutrino Oscillation Parameters with KamLAND. *Phys. Rev. Lett.*, 100:221803, 2008.

[5] Abe, K., et al. Indication of Electron Neutrino Appearance from an Accelerator-produced Off-axis Muon Neutrino Beam. *Phys. Rev. Lett.*, 107:041801, 2011.

[6] Abe, Y., et al. Indication of Reactor $\bar{\nu}_e$ Disappearance in the Double Chooz Experiment. *Phys. Rev. Lett.*, 108:131801, 2012.

[7] An, F. P., et al. Observation of electron-antineutrino disappearance at Daya Bay. *Phys. Rev. Lett.*, 108:171803, 2012.

[8] Ahn, J. K., et al. Observation of Reactor Electron Antineutrino Disappearance in the RENO Experiment. *Phys. Rev. Lett.*, 108:191802, 2012.

[9] Adamson, P., et al. Electron neutrino and antineutrino appearance in the full MINOS data sample. *Phys. Rev. Lett.*, 110:171801, 2013.

[10] Forero, D. V., Tortola, M. and Valle, J. W. F. Neutrino oscillations refitted.*Phys. Rev. D*, 90:093006, 2014.

[11] Ade, P. A. R., et al. [PLANCK collaboration], Planck 2013 results. XVI. Cosmological parameters. *Astron.Astrophys.*, 571:A16, 2014.

[12] Ade, P. A. R., et al. [Planck Collaboration], Planck 2015 results-XIII. cosmological parameters. *Astron.Astrophys.*, 594:A13, 2016.

[13] Minkowski, P. $\mu \to e\gamma$ at a Rate of One Out of 10^9 Muon Decays? *Phys. Lett. B*, 67:421, 1977.

[14] Mohapatra, R. N. and Senjanovic, G. Neutrino Mass and Spontaneous Parity Non-conservation,.Phys. Rev. Lett., 44:912, 1980.

[15] Schechter, J. and Valle, J. W. F. *Neutrino Masses in SU(2) x U(1)Theories. Phys. Rev. D*, 22:2227, 1980.

[16] Mohapatra, R. N. and Senjanovic, G. Neutrino Masses and Mixings in Gauge Models with Spontaneous Parity Violation. *Phys. Rev. D*, 23:165, 1981.

[17] Lazarides, G., Shafi, Q. and Wetterich, C. Proton Lifetime and Fermion Masses in an SO(10) Model.*Nucl. Phys. B*, 181:287, 1981.

[18] Schechter, J. and Valle, J. W. F. Neutrino Decay and Spontaneous Violation of Lepton Number. *Phys. Rev. D*, 25:774, 1982.

[19] Foot, R., Lew, H., He, X. G., and Joshi, G. C. Seesaw Neutrino Masses Induced by a Triplet of Leptons. *Z. Phys. C*, 44:441, 1989.

[20] Ma, E. Pathways to naturally small neutrino masses, *Phys. Rev. Lett.*, 81:1171, 1998.

[21] Mohapatra, R. N., Valle, J. W. F. Neutrino mass and baryon number non conservation in super string models. *Phys. Rev. D*, 34(5):1642, 1986.

[22] Bernabeu, J., Santamaria, A., Vidal, J., Mendez, A., and Valle, J. W. F. Lepton flavour non conservation at high energies in a super string inspired standard model. *Phys. Lett. B*, 187:303, 1987.

[23] Pati, J. C. and Salam, A. Lepton Number as the Fourth Color. *Phys.Rev.D*, 10:275, 1974 .

[24] Mohapatra, R. N. and Pati, J. C. Left-Right Gauge Symmetry and an Isoconjugate Model of CP Violation. *Phys. Rev. D*, 11:566, 1975.

[25] Mohapatra R. N. and Pati, J. C. A Natural Left-Right Symmetry. *Phys.Rev.D*, 11:2558, 1975.

[26] Senjanovic, G. and Mohapatra R. N. Exact Left-Right Symmetry and Spontaneous Violation of Parity. *Phys.Rev.D*, 12:1502, 1975.

[27] Mohapatra, R. N., Paige, F. E. and Sidhu, D. P. Symmetry Breaking and Naturalness of Parity Conservation in Weak Neutral Currents in Left-Right Symmetric Gauge Theories. *Phys. Rev. D*, 17:2462, 1978.

[28] Mohapatra, R. N. and Pati, J. C. A Natural Left-Right Symmetry. *Phys. Rev. D*, 11:2558, 1975.

[29] Rodejohann, W. Neutrino-less Double Beta Decay and Particle Physics. *Int. J. Mod. Phys.*, E20:1833-1930, 2011.

[30] Bilenky, S. M., Giunti, C. Neutrinoless double beta decay-a brief review. *Mod. Phys. Lett.*, A27 (13):1230015, 2012.

[31] Schechter, J. and Valle, J. W. F. Neutrinoless double-Îš decay in $SU(2)\times U(1)$ theories. *Phys. Rev. D*, 25:2951, 1982.

[32] Schwingenheuer, B. Searches for neutrinoless double beta decay. *arXiv:1201.4916*, 2012.

[33] Bilenky, S. M., Hosek, J. and Petcov, S.T. On Oscillations of Neutrinos with Dirac and Majorana. *Phys. Lett. B*, 94:495, 1980.

[34] Mohapatra, R. N. and Rodejohann, W. Scaling in the neutrino mass matrix. *Phys. Lett. B*, 644:59, 2007.

[35] Garfagnin, A. Neutrinoless double beta decay experiments. *Int. J. Mod. Phys. Conf. Ser.*, 31:1460286, 2014.

[36] Ostrovskiy, I, O'Sullivan, K. Search for neutrinoless double beta decay. *Mod. Phys. Lett.*, A31:1630017, 2016.

[37] Gando, A., et al. Search for Majorana Neutrinos near the Inverted Mass Hierarchy Region with KamLAND-Zen. *Phys. Rev. Lett.*, 117:082503, 2016.

[38] Agostini, M., et al. [GERDA Collaboration], Search of Neutrinoless Double Beta Decay with the GERDA Experiment. *Nuclear and Particle Physics Proceedings*, (273-275):1876-1882, 2016.

[39] Harrison, P. F., Perkins, D. H. and Scott, W. G. Tri-bimaximal mixing and neutrino oscillation data. *Phys. Lett. B*, 530(1): 167-173, 2002.

[40] Harrison, P. F. and Scott, W. G. Symmetries and generalizations of tri-bimaximal mixing. *Phys. Lett. B*, 535(1):163-169, 2002.

[41] Xing, Z. Z. Nearly tri-bimaximal neutrino mixing and CP violation. *Phys. Lett. B*, 533(1): 85-93, 2002.

[42] Harrison, P. F. and Scott, W. G. $\mu - \tau$ reflection symmetry in lepton mixing and neutrino oscillations. *Phys. Lett. B*, 547 (3):219-228, 2002.

[43] Vissani, F. A. study of the scenario with nearly degenerate Majorana neutrinos. *arXiv:9708483*, 1997.

[44] Barger, V., et al. Bi-maximal mixing of three neutrinos. *Phys. Lett. B*, 437(1):107-116, 1998.

[45] Albright, C. H., Dueck, A. and Rodejohann, W. Possible alternatives to tri-bimaximal mixing. *Eur. Phys. J., C*, 70(4):1099-1110, 2010.

[46] Datta, A., Ling, F., and Raymond, P. Correlated hierarchy, Dirac masses and large mixing angles. *Nucl. Phys. B*, 671:383-400, 2003.

[47] Kajiyama, Y., Raidal, M. and Strumia, A. Golden ratio prediction for solar neutrino mixing. *Phys. Rev. D*, 76 (11):117301, 2007.

[48] Everett, L. L. and Stuart, A. J. Icosahedral (A_5) family symmetry and the golden ratio prediction for solar neutrino mixing. *Phys. Rev. D*, 79:085005, 2009.

[49] Borah, D., Deviations from Tri-Bimaximal Neutrino Mixing Using Type II Seesaw. *Nucl. Phys. B*, 876(2):575-586, 2013.

[50] Cirigliano, V., Kurylov, A., Ramsey-Musolf, M. J. and Vogel, P. Lepton flavor violation without supersymmetry. *Phys. Rev. D*, 70:075007, 2004.

[51] Barry, J. and Rodejohann, W., Lepton number and flavour violation in TeV-scale left-right symmetric theories with large left-right mixing. *JHEP*, 09:153, 2013.

[52] Borah, D. and Dasgupta, A., Charged lepton flavour violcxmation and neutrinoless double beta decay in left-right symmetric models with type I+II seesaw. *JHEP*, 07:022, 2016.

[53] Abbas, M and Khalil, S. Neutrino masses, mixing and leptogenesis in TeV scale B- L extension of the standard model. *JHEP*, 04:056, 2008.

[54] Dev, PS and Zhang, Y. Displaced vertex signatures of doubly charged scalars in the type-II seesaw and its left-right extensions. *JHEP*, 10:199, 2018.

[55] Ge, S.F. and Lindner, M. and Patra, S. New physics effects on neutrinoless double beta decay from right-handed current. *JHEP*, 10:077, 2015.

[56] Barry, J. and Rodejohann, W. Lepton number and flavour violation in TeV-scale left-right symmetric theories with large left-right mixing. *JHEP*, 09:153, 2013.

[57] Awasthi, R. L. and Dev, P.S. B. and Mitra, M. Implications of the diboson excess for neutrinoless double beta decay and lepton flavor violation in TeV scale left-right symmetric model. *Phys. Rev. D*, 93(1):011701, 2016.

[58] Chakrabortty, J. and Devi, H.Z. and Goswami, S. and Patra, S. Neutrinoless double-β decay in TeV scale Left-Right symmetric models. *JHEP*, 08:008, 2012.

[59] Borah, D. and Dasgupta, A. Neutrinoless double beta decay in type I+ II seesaw models. *JHEP*, 11:208, 2015.

[60] Parida, M.K. and Patra, S. Left-right models with light neutrino mass prediction and dominant neutrinoless double beta decay rate. *Phys. Lett. B*, 718(4-5):1407-1412, 2013.

[61] Bambhaniya, G., Dev, P. S. B and Goswami, S., Mitra, M. The scalar triplet contribution to lepton flavour violation and neutrinoless double beta decay in left-right symmetric model. *JHEP*, 04:046, 2016.

[62] Lindner, M., Rodejohann, W. Large and almost maximal neutrino mixing within the type II see-saw mechanism. *JHEP*, 05:089, 2007.

[63] Rodejohann, W. Type II See-Saw Mechanism, Deviations from Bimaximal Neutrino Mixing and Leptogenesis. *Phys.Rev. D*, 70:073010, 2004.

[64] Chakraborty, J., Devi, H. Z., Goswami, S., Patra, S. Neutrinoless double-β decay in TeV scale Left-Right symmetric models. *JHEP*, 08:008, 2012.

[65] Borah, D. and Dasgupta, A. Neutrinoless double beta decay in type I+ II seesaw models. *JHEP*, 11:208, 2015.

[66] Mohapatra, R. N. and Vergados, J.D. A New Contribution to Neutrinoless Double Beta Decay in Gauge Models. *Phys.Rev.Lett.*, 47: 1713-1716, 1981.

[67] Pich, A. The Standard Model of Electroweak Interactions. *arXiv:hep-ph/0502010*, 2005.

[68] Borah, D., Patra, S., Sarkar, U. TeV scale Left Right Symmetry with spontaneous D-parity breaking. *Phys. Rev. D*, 83:035007, 2011.

[69] Hirsch, M., Klapdor-Kleingrothaus, H.V., Panella, O. Double beta decay in left-right symmetric models. *Phys. Lett. B*,374: 7-12, 1996.

[70] Danamik, A. Nonzero θ_{13} and CP violation from broken $\mu - \tau$ symmetry. *Journal of Phys:Conference Series*, 539:012012, 2014.

[71] Awasthi, R. L., Dev, P. S. B. and Mitra, M. Implications of the Diboson Excess for Neutrinoless Double Beta Decay and Lepton Flavor Violation in TeV Scale Left Right Symmetric Model. *Phys. Rev. D*, 93:011701, 2016.

[72] Baldini, A. M., et al. [MEG collaboration], Search for the lepton flavour violating decay $\mu \to e\gamma$ with the full dataset of the MEG experiment. *Eur. Phys. J. C*, 76(8):434, 2016.

[73] Bellgardt, U., et al. [SINDRUM collaboration], Search for the Decay $\mu \to 3e$. *Nucl. Phys. B*, 299:1-6, 1988.

[74] Blonde, A., et al. Research Proposal for an Experiment to Search for the Decay $\mu \to 3e$. *arXiv:1301.6113*, 2013.

[75] Gouvea, A. and Vogel, P., Lepton Flavor and Number Conservation, and Physics Beyond the Standard Model. *Nucl. Phys. B*, 71: 75-92, 2013.

[76] Mitra, M., et al. Neutrino Jets from High-Mass WR Gauge Bosons in TeV-Scale Left-Right Symmetric Models. *Phys. Rev. D*, 94:095016, 2016.

[77] Borah, D. and Dasgupta, A. Neutrinoless Double Beta Decay in Type I+II Seesaw Models. *JHEP*, 11:208, 2015.

[78] Kotila, J. and Iachello, F. Phase-space factors for double-β decay. *Phys. Rev. C*, 85:034316, 2012.

[79] Bhupal Dev, P. S., Goswami, S. and Mitra, M. TeV Scale Left-Right Symmetry and Large Mixing Effects in Neutrinoless Double Beta Decay. *Phys. Rev. D*, 91:113004, 2015.

[80] Pantis, G., Simkovik, F., Vergados, J. D. and Faessler, A. Neutrinoless Double Beta Decay within QRPA with Proton-Neutron Pairing. *Phys. Rev. C*, 53:695, 1996.